J M M
Journal of Mechanics and MEMS
Special Issue dedicated to Prof. K Y Ye edited by Z M Ye, P Liu and B Sun

ISSN: 0974-8407

9(2) 2017: pp. 409-420

PIEZOELECTRIC LAYERS APPLICATION TO CONTROL OF PULL-IN VOLTAGE AND NATURAL FREQUENCY OF AN ELECTROSTATICALLY ACTUATED MICROPLATE

Ghader Rezazadeh[1], Soheil Talebian[2], Hadi Yagubizade[3] and Yashar Alizadeh[4]

ABSTRACT

In the present article, an improved model to control the pull-in voltage and natural frequency of the electrostatically actuated microplate using of surface-bonded piezoelectric layers has been presented. This work consists of two major parts. In the first part, static instability and the effect of negative and positive applied voltage to the piezoelectric layers on it for a microplate subjected to non-linear electrostatic pressure has been investigated considering the effect of stretching and residual stresses. To this end, the nonlinear integro-differential governing equation has been derived using Kirchhoff thin plate theory and has been solved using Step-by-Step Linearization Method and applying finite difference method to the linearized differential equation. In the second part in order to study natural or eigen frequency of the system the small vibrations about the equilibrium position have been studied. The linear governing differential equation has been solved by using of a Galerkin based reduced order model and the natural frequencies of the micro plate have been calculated. The obtained results show that by applying different voltage to the piezoelectric layers, the pull-in voltage and natural frequency of the system can be controlled and tuned easily.

Keywords: Piezoelectric Layers, Pull-In Voltage, Natural Frequency, Step by Step Linearization Method

1. INTRODUCTION

Thanks to recent advances in the technology of microelectromechanical systems (MEMS) and nanoelectromechanical systems (NEMS), micro and nano sensors and actuators driven by an electrostatic force become objects of intensive study owing to their merits of small size, batch production, low-energy consumption, and compatibility with the integrated circuits (ICs). These micro-devices are key components of many devices and commonly seen in various structures such as micro-pumps [1-3], micro-mirrors [4], accelerometer [5], pressure sensors [6-7] and etc. For this reason further advances in MEMS and NEMS design are very important and require more and deeper investigation and understanding of basic phenomena at the micro and nano scale devices.

Electrically actuated microplates are the main component in micropumps, micromirrors, microphones, and many microsensors [8-11]. Application of these MEMS devices are spread over biotechnology, image processing, automotive, chemical, food, and mining industries. An electrically actuated microplate forms one side of a variable capacity air-gap capacitor is shown in Fig. 1. An electrostatic field is created by applying a potential difference between the microplate and a fixed electrode. As the electrostatic force deforms the microplate, the electrostatic force itself changes with the plate deflection, resulting in coupling of the electrical and mechanical forces. The applied electrostatic load has an upper limit beyond which the mechanical restoring force of the microplate can no longer resist the electrostatic force, thereby leading to the collapse of the structure. This structural instability phenomenon is a divergence instability and in the MEMS is known as 'pull-in', and the critical voltage associated with it, is called the 'pull-in voltage'. The mathematical analysis of these systems started in the late 1960s with the

1,2,3. Mechanical Engineering Department, Urmia University, Urmia, Iran

4. Mechanical Engineering Department, Khoy Azad University, Khoy, Iran, *E-mail: g.rezazadeh@urmia.ac.ir*

pioneering work of H. C. Nathanson and his coworkers [12] who constructed and analyzed a mass-spring model of electrostatic actuation, and offered the first theoretical explanation of pull-in instability. At roughly the same time, G. I. Taylor [13] studied the electrostatic deflection of two oppositely charged soap films, and he predicted that when the applied voltage was increased beyond a certain critical voltage, the two soap films would touch together. While Taylor was interested in the electrostatic deflection of soap films, the small-aspect ratio model introduced in his work is the basis of many modern studies of electrostatic deflections in MEMS and NEMS. Since Nathanson and Taylor's seminal work, numerous investigators have analyzed and developed mathematical models of electrostatic actuation in attempts to understand further and control pull-in instability [14-15].

Electrostatic micro devices are usually operated at their resonant frequencies, which will give the maximum displacement amplitude and the highest operating efficiency [16-17]. As a large number of micro devises is operated at resonance, the prediction of the natural frequencies is a key factor in the design phase. For coupled microelectromechanical systems, the natural frequencies shift with increasing applied voltage. This characteristic turns possible for example to tune an operating frequency with an applied voltage [18]. Forecasting this voltage dependent frequency behavior is thus very worthy.

Fully clamped microplates have very high natural frequencies. Previous works on the frequency analysis of the microplates used very simplified models in which microplates are assumed as lumped model, however, these devices must be modeled to continuum structures because these devices assumed as rigid body in previous works are generally deformable. Moreover, in real situations, the electrostatic field and the elastic deformation field of the system are 3-dimentionally coupled. An advanced numerical approach, which can treat continuous fields, is used only in the calculation of the electrostatic force applied on the device [19]. In order to accuracy predict the behavior of the real system, the analysis of the coupled fields in 3-D continuous system for evaluating the effects of electrostatic field on natural frequency is necessary.

Nayfeh *et al.* have investigated a nonlinear modeling of the annular plates [20], clamped circular plates [21], and simply supported rectangular plates [22]. They determined the static deflection using both a numerical shooting technique [20] and a reduced order model [21-22]. Because the shooting method is an iterative procedure, where a solution is assumed over the whole domain and then corrected iteratively, it is computationally expensive. Further, the shooting suffers from the stiffness of the equations and hence might become unstable, especially as the pull-in is approached. Reduced order models, on the other hand, provide a possible solution to these problems.

Considering the fabrication sequence of MEM actuators, the residual stress is very important and inevitable to the device. Residual stress due to the mismatch of both thermal expansion coefficient and crystal lattice period between substrate and thin film is unavoidable in surface micromachining techniques, so that accurate and reliable data of residual stress is crucial to the proper design of the MEMS devices concerned with the techniques [23]. Therefore the residual stress is an attractive research topic in the development of the microsystems technology. Effect of Residual stress has been researched on micro-beams by several researches such as Gh. Rezazadeh et al. [14] and L. X. Zhang and Y. P. Zhao [24] but this effect and axial stress due to stretching in rectangular microplates has not been researched enough.

The applications of the smart materials in engineering structures have drawn serious attention recently. The piezoelectric materials are light and able to provide rapid response through electro-mechanical coupling. Such as shape control of structures [25], acoustic wave excitation [26] and structures health monitoring [27]. However, the research on using piezoelectric materials to enhance the controlling of MEMS plate based structures behavior such as pull-in voltage has not attracted much attention from the scientific community.

Therefore, in this paper, based on the characteristic of the piezoelectric materials, an improved distributed model is used to obtain the deflection and divergence instability of the electrostatically actuated microplates by means of surface-bonded piezoelectric layers. An isotropic thin rectangular piezoelectric layers and flexible micro plate has been considered. The deflection and the pull-in phenomenon of the plate using SSLM and applying FDM have been investigated. Then we studied on the small vibrations around the equilibrium position and obtained the dynamic linear partial differential equation of the micro plate motion. The Galerkin procedure was used to generate the reduced order model and discretize the governing equation to calculate the natural frequency of the system. The obtained results show that pull-in voltage and natural frequency of the micro plate can be controlled successfully by using of piezoelectric layers.

2. MODEL DESCRIPTION AND ASSUMPTIONS

As it is shown in the Fig. 1, the upper part of this device consists of a rectangular plate with thickness h, length a, width b and isotropic with Young's modulus E, Poisson's ratio υ and material density ρ which surface-bonded with two piezoelectric layers. Each piezoelectric layer has thickness h_1, isotropic with Young's modulus E_p, Poisson's ratio υ_p and equivalent piezoelectric coefficients $\bar{e}_{31}$, $\bar{e}_{32}$ in x and y directions, respectively. It is clamped along its all boundaries and the lower part which is entitled ground plate, attached to a rigid substrate. When the voltage is applied between these plates, the flexible plate is deflected toward the ground plate.

3. MATHEMATICAL MODELING

3.1. Static Behavior of Electrostatically Actuated Multilayer Plate

The governing equation for the multilayer plate subjected to nonlinear electrostatic pressure, shown in figure 1, can be expressed as [28]:

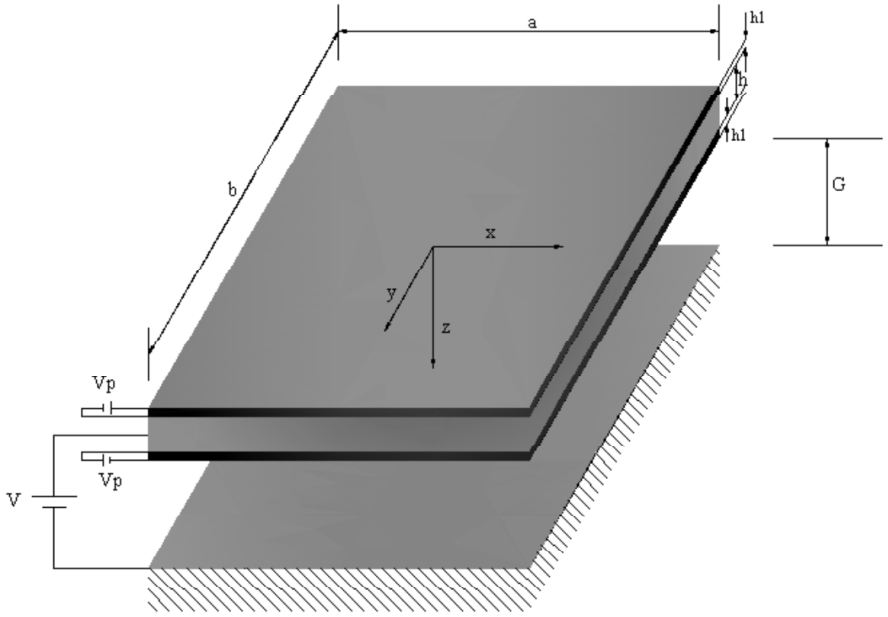

Figure 1: Schematic View of the Device

$$D_t\left(\frac{\partial^4 w_b}{\partial x^4}+2\frac{\partial^4 w_b}{\partial x^2\partial y^2}+\frac{\partial^4 w_b}{\partial y^4}\right)=q(x,y) \tag{1}$$

where $w_b(x, y)$ is the deflection of the plate and D_t is the transformed flexural rigidity of laminated composite plate and in symmetric proposed model because of small thickness of piezoelectric layers , it can be expressed as follow:

$$D_t=\frac{Eh^3}{12(1-\upsilon^2)}+\frac{E_p h h_1}{(1-\upsilon_p^2)}\left[\frac{h}{2}+h_1\right] \tag{2}$$

Electrostatic pressure is derived from a parallel-plate approximation respect to an applied voltage. The electrostatic pressure applied per unit area of the plate can be written as:

$$q(x,y)=\frac{\varepsilon_0 V^2}{2(G-w_b)^2} \tag{3}$$

where V is the applied voltage between the movable and the ground plates on the fixed substrate, G is the initial gap between the movable/fixed plates and ε_0 is the permittivity of air. The boundary conditions for the rectangular plate

clamped at all edges are:

$$w_b\left(-\frac{a}{2},y\right)=w\left(\frac{a}{2},y\right)=0,\ \left(\frac{\partial w_b}{\partial x}\right)\Big|_{x=-\frac{a}{2},\frac{a}{2}}=0 \tag{4}$$

$$w_b\left(x,-\frac{b}{2}\right)=w\left(x,\frac{b}{2}\right)=0,\ \left(\frac{\partial w_b}{\partial y}\right)\Big|_{y=-\frac{b}{2},\frac{b}{2}}=0 \tag{5}$$

3.2. Residual Stress Effect

Residual stress due to the mismatch of both thermal expansion coefficient and crystal lattice period between substrate and thin film is unavoidable in surface micromachining techniques. The residual stresses can be modeled as follow [29]:

$$T_x^r=\sigma_x^r h \tag{6}$$

$$T_y^r=\sigma_y^r h \tag{7}$$

3.3. Stretching Stress Effect

The bringing out equation for considered model is imperfect because when the electrostatic pressure applied to the flexible plate, the plate deflects and because of clamped boundary conditions some biaxial stresses are created in the *x* and y directions. So for accurate modeling of microplates with clamped boundary conditions axial or stretching stresses must be considered. In every assumed line in *x* or *y* direction, the actual length along the center line of the plate is calculated by integrating the arc length *ds* along the assumed curved line in the plate based on the cubic shape functions for small angle plate deflection :

$$L_x'(y)=\int_0^a ds_x\approx\int_0^a\sqrt{1+\left(\frac{\partial w_b}{\partial x}\right)^2}\,dx, \tag{8}$$

$$L_y'(x)=\int_0^b ds_y\approx\int_0^b\sqrt{1+\left(\frac{\partial w_b}{\partial y}\right)^2}\,dy, \tag{9}$$

Considering $L_x, L_y \succ\succ w_b$, hence $\left(\partial w_b/\partial x\right)^2 \prec\prec 1,$ and $\left(\partial w_b/\partial y\right)^2 \prec\prec 1,$ as a result, the elongation per unit length is approximately given by:

$$\varepsilon_x^a\cong\frac{1}{2a}\int_0^a\left(\frac{\partial w_b}{\partial x}\right)^2 dx, \tag{10}$$

$$\varepsilon_y^a\cong\frac{1}{2b}\int_0^b\left(\frac{\partial w_b}{\partial y}\right)^2 dy, \tag{11}$$

The stretching forces per unit width of the undeformed plate are:

$$T_x^a=\sum_{i=1}^{3}\sigma_{ix}^a(t_{i+1}-t_i)=\sum_{i=1}^{3}\frac{E_i(t_{i+1}-t_i)}{1-\upsilon_i^2}\left(\frac{1}{2a}\int_0^a\left(\frac{\partial w_b}{\partial x}\right)^2 dx+\upsilon_i\frac{1}{2b}\int_0^b\left(\frac{\partial w_b}{\partial y}\right)^2 dy\right) \tag{12}$$

$$T_y^a=\sum_{i=1}^{3}\sigma_{iy}^a(t_{i+1}-t_i)=\sum_{i=1}^{3}\frac{E_i(t_{i+1}-t_i)}{1-\upsilon_i^2}\left(\frac{1}{2b}\int_0^b\left(\frac{\partial w_b}{\partial y}\right)^2 dy+\upsilon_i\frac{1}{2a}\int_0^a\left(\frac{\partial w_b}{\partial x}\right)^2 dx\right) \tag{13}$$

where t_i is the distance of the $i-th$ surface of the multilayer plate from midplane.

3.4. Piezoelectric Layers Force

The stress in the piezoelectric layers considering uniform electric field created by applied voltage can be expressed as [30]:

$$\sigma_x^p = \frac{E}{1-\upsilon_p^2}(\varepsilon_x + \upsilon\varepsilon_y) - \overline{e}_{31}E_z \tag{14}$$

$$\sigma_y^p = \frac{E}{1-\upsilon_p^2}(\upsilon\varepsilon_x + \varepsilon_y) - \overline{e}_{32}E_z \tag{15}$$

where E_z is the electric field in the piezoelectric layers and equal to $E_z = V_p / h_1$. If the piezoelectric layers are placed symmetrically and poled in the transverse direction of the plate, applying equal voltages V_p to the upper and lower piezoelectric layers will induce tensile or compressive mechanical stresses on the plate if complete bonding is assumed, meanwhile, the following equation can be obtained [14]:

$$\begin{aligned} T_x^p = &\int_{-h/2-h_1}^{-h/2}\left(-\frac{E}{1-\upsilon_p^2}\left(z\frac{\partial^2 w_b}{\partial x^2} + \upsilon_p z\frac{\partial^2 w_b}{\partial y^2}\right) - \overline{e}_{31}E_z\right)dz + \\ &\int_{h/2}^{h/2+h_1}\left(-\frac{E}{1-\upsilon_p^2}\left(z\frac{\partial^2 w_b}{\partial x^2} + \upsilon_p z\frac{\partial^2 w_b}{\partial y^2}\right) - \overline{e}_{31}E_z\right)dz = -2h_1E_z\overline{e}_{31} = -2\overline{e}_{31}v_p \end{aligned} \tag{16}$$

$$\begin{aligned} T_y^p = &\int_{-h/2-h_1}^{-h/2}\left(-\frac{E}{1-\upsilon_p^2}\left(\upsilon_p z\frac{\partial^2 w_b}{\partial x^2} + z\frac{\partial^2 w_b}{\partial y^2}\right) - \overline{e}_{32}E_z\right)dz + \\ &\int_{h/2}^{h/2+h_1}\left(-\frac{E}{1-\upsilon_p^2}\left(\upsilon_p z\frac{\partial^2 w_b}{\partial x^2} + z\frac{\partial^2 w_b}{\partial y^2}\right) - \overline{e}_{32}E_z\right)dz = -2h_1E_z\overline{e}_{32} = -2\overline{e}_{32}v_p \end{aligned} \tag{17}$$

Such tensile and compressive force applied by the piezoelectric layer, depends on the direction of the electric field, which can be used to control the pull-in voltage or shift resonant or natural frequency of the microplate to upward or downward.

Now by considering all of the above effects, the governing non-linear equation for the multilayer plate subjected to nonlinear electrostatic pressure can be rearranged as follow:

$$D_t\left(\frac{\partial^4 w_b}{\partial x^4} + 2\frac{\partial^4 w_b}{\partial x^2\partial y^2} + \frac{\partial^4 w_b}{\partial y^4}\right) - \left(T_x^r + T_x^a + T_x^p\right)\frac{\partial^2 w_b}{\partial x^2} - \left(T_y^r + T_y^a + T_y^p\right)\frac{\partial^2 w_b}{\partial y^2} = \frac{\varepsilon_0 V^2}{2(G-w_b)^2} \tag{18}$$

3.5. Small Vibrations of Electrostatically Deflected Micro Plate

With solving the Eq. (18) numerically, the deflection of plate can be obtained and the equilibrium position of micro plate can be identified. To ensure the stability or instability of the plate in the equilibrium position and also to study resonant frequency of the micro plate, the small vibrations about this position are studied. The deflection of microplate can be written as the sum of following two terms:

$$w(x, y, t) = w_b(x, y) + \varepsilon(x, y, t) \tag{19}$$

where $w_b(x, y)$ is the deflection of the micro plate in equilibrium position due to applied voltage, introduced in Eq. (18) and $\varepsilon(x, y, t)$ is plate small oscillations about its equilibrium position. The linear equation of small oscillations about equilibrium position with using the calculus of variation theory and Taylor's series expansion about w_b and applying the truncation to the first order of it in order to linearize the electrostatic force, can be written as:

$$L(\varepsilon(x,y,t)) = D_t\left(\frac{\partial^4\varepsilon}{\partial x^4} + 2\frac{\partial^4\varepsilon}{\partial x^2\partial y^2} + \frac{\partial^4\varepsilon}{\partial y^4}\right) - \left(T_x^r + T_x^a + T_x^p\right)\frac{\partial^2\varepsilon}{\partial x^2}$$
$$-\left(T_y^r + T_y^a + T_y^p\right)\frac{\partial^2\varepsilon}{\partial y^2} - \frac{\varepsilon_0 V^2}{(G-w_b)^3}\varepsilon + \rho h\left(\frac{\partial^2\varepsilon}{\partial t^2}\right) = 0 \tag{20}$$

$\varepsilon(x, y, t)$ satisfies the same boundary conditions as $w_b(x, y)$. It must be noted that the variation of the stretching terms (T_x^a , T_y^a) due to small value of $\varepsilon(x, y, t)$ can be neglected.

4. NUMERICAL SOLUTION

4.1. Response to Static Loading

Due to the non-linearity of governing equation created by electrostatic pressure, an analytical solution is impractical to obtain and a numerical solution is sought. The search for a solution of the electrostatic deflections problems by numerical technique currently produces cost effective design and analysis for a variety of problems. The choice of difference operators plays a major role in accuracy solutions. An account of the way out of the non-linearity problem was utilized with the linearization method for charging the governing equation into a linear equation. Because of the considerable value of w_b respect to initial gap especially when the applied voltage is increased, the linearization with respect to w_b may cause considerable errors. Therefore, to minimize the value of errors, the method of step-by-step increasing the applied voltage is proposed and the governing equation has been linearized at the each step [14].

By using of SSLM, it is supposed that the w_b^k, is the displacement of plate due to the applied voltage V^k. Therefore, by increasing the applied voltage to a new value, the displacement can be written as:

$$w_b^{k+1} = w_b^k + \delta w_b = w_b^k + \psi(x,y) \tag{21}$$

when

$$V^{k+1} = V^k + \delta V \tag{22}$$

By considering small value of δV, it is expected that the ψ would be small enough, hence by using of calculus of variation theory and Taylor's series expansion about w_b^k, and applying the truncation to first order of it for suitable value of δV, it is possible to obtain desired accuracy. Therefore the linearized form of Eq. (18) can be written as

$$D_t\left[\frac{\partial^4\psi}{\partial x^4} + 2\frac{\partial^4\psi}{\partial x^2\partial y^2} + \frac{\partial^4\psi}{\partial y^4}\right] - \left[T_x^r + T_x^p + \left(T_x^a\right)^k + \delta T_x^a\right]\frac{\partial^2\psi}{\partial x^2} - \delta T_x^a\left(\frac{\partial^2 w_b}{\partial x^2}\right)$$
$$-\left[T_x^r + T_x^p + \left(T_x^a\right)^k + \delta T_x^a\right]\frac{\partial^2\psi}{\partial y^2} - \delta T_y^a\left(\frac{\partial^2 w_b}{\partial y^2}\right) - \frac{\varepsilon_0\left(V^k\right)^2}{\left(G - w_b^k\right)^3}\psi = \frac{\varepsilon_0 V^k \delta V}{\left(G - w_b^k\right)^2} \tag{23}$$

Where δT_x^a and δT_y^a are the variations of hardening or stretching term and can be defined as:

$$\delta T_x^a = \sum_{i=1}^{3}\frac{E_i(t_{i+1} - t_i)}{1-\upsilon_i^2}\left(\frac{1}{a}\int_0^a\left(\frac{\partial^2 w_b^k}{\partial x^2}\right)\psi(x,y)dx + \upsilon_i\frac{1}{b}\int_0^b\left(\frac{\partial^2 w_b^k}{\partial y^2}\right)\psi(x,y)dy\right) \tag{24}$$

$$\delta T_y^a = \sum_{i=1}^{3}\frac{E_i(t_{i+1} - t_i)}{1-\upsilon_i^2}\left(\frac{1}{b}\int_0^b\left(\frac{\partial^2 w_b^k}{\partial y^2}\right)\psi(x,y)dy + \upsilon_i\frac{1}{a}\int_0^a\left(\frac{\partial^2 w_b^k}{\partial x^2}\right)\psi(x,y)dx\right) \tag{25}$$

Implying any numerical method and imposing the boundary conditions, the Eq. (23) can be discretized. By using of central finite difference formula due to a rectangular mesh with constant subdivisions Δx and Δy characteristics and by solving linear system of obtained algebraic equation equations, the $\psi(x, y)$ can be achieved at a given applied voltage.

4.2. Eigen Frequency Analysis

To solve the Eq. (20) various forms of discretization can be used. The major discretization methods that can be applied directly to differential equation are finite difference methods and weighted residual methods or Galerkin method. In these methods the infinite set of numbers representing the unknown function or functions is replaced by a finite number of unknown parameters, and this process in general, requires some form of approximation.

In the present article the weighted residual methods was used to discretize the equation. Therefore, $\varepsilon(x, y, t)$ can be expanded with respect to basis functions as follows:

$$\varepsilon(x,y,t)=\sum_{m=1}^{\infty}\sum_{n=1}^{\infty}U_{nm}(t)\phi_n(x)\varphi_m(y) \tag{26}$$

Where the $\phi_n(x)$ and $\varphi_m(y)$ are the basis functions, satisfy the existing geometrical boundary conditions. To generate a reduced-order model (ROM) by discretizing Eq. (20) into a finite-degree-of-freedom system, initially, an approximate solution is considered:

$$\varepsilon_{NM}(x,y,t)=\sum_{m=1}^{M}\sum_{n=1}^{N}U_{nm}(t)\phi_n(x)\varphi_m(y) \tag{27}$$

Then the Galerkin procedure can be used. In this procedure, with substituting Eq. (27) into Eq. (20) and multiplying by $\phi_n(x)$ and $\varphi_m(y)$ as weighting functions and integrating the outcome from $x = 0$ to a and $y = 0$ to b, the reduced-order model is generated:

$$\int_0^a\int_0^b \phi_i(x)\varphi_j(y)L(\varepsilon_{NM}(x,y,t))dxdy=0 \quad i=1,\ldots,N,\ j=1,\ldots,M \tag{28}$$

By introducing the following parameters:

$$K_{ijnm}^{(m)}=\int_0^a\int_0^b \phi_i(x)\varphi_j(y)\begin{pmatrix} D_t\phi_n^4(x)\varphi_m(y)+D_t 2\phi_n^2(x)\varphi_m^2(y)+D_t\phi_n(x)\varphi_m^4(y) \\ -\left(T_x^r+T_x^a\right)\phi_n^2(x)\varphi_m(y)-\left(T_y^r+T_y^a\right)\phi_n(x)\varphi_m^2 \end{pmatrix}dxdy$$
$$i=1,\ldots,N\ ,\ j=1,\ldots,M\ ,\ n=1,\ldots,\mathrm{N}\ ,\ m=1,\ldots,M \tag{29}$$

$$K_{ijnm}^{(p)}=\int_0^a\int_0^b \phi_i(x)\varphi_j(y)\left(T_x^p\phi_n^2(x)\varphi_m(y)+T_y^p\phi_n(x)\varphi_m^2\right)dxdy$$
$$i=1,\ldots,N\ ,\ j=1,\ldots,M\ ,\ \mathrm{n}=1,\ldots,N\ ,\ m=1,\ldots,M \tag{30}$$

$$K_{ijnm}^{(e)}=\int_0^a\int_0^b \phi_i(x)\varphi_j(y)\left(\frac{\varepsilon_0 V^2\phi_n(x)\varphi_m(y)}{(G-w_b)^3}\right)dxdy$$
$$i=1,\ldots,N\ ,\ j=1,\ldots,M\ ,\ n=1,\ldots,N\ ,\ m=1,\ldots,M \tag{31}$$

$$M_{ijnm}=\int_0^a\int_0^b \rho h\phi_i(x)\varphi_j(y)\left(\phi_n(x)\varphi_m(y)\right)dxdy$$
$$i=1,\ldots,N\ ,\ j=1,\ldots,M\ ,\ n=1,\ldots,N\ ,\ m=1,\ldots,M \tag{32}$$

and substituting them into Eq. (28), a set of $N \times M$ ordinary differential equations with respect to time can be obtained as follow:

$$\sum_{m=1}^{M}\sum_{n=1}^{N} M_{ijnm}\ddot{U}_{nm}(t)+\sum_{m=1}^{M}\sum_{n=1}^{N}\left\{K_{ijnm}^{(m)}-K_{ijnm}^{(p)}-K_{ijnm}^{(e)}\right\}U_{nm}(t)=0 \quad i=1,\ldots,N \quad j=1,\ldots,M \tag{33}$$

With substituting the following equation,

$$U_{nm}(t)=a_{nm}e^{i\omega t} \tag{34}$$

into Eq. (33), we have:

$$\sum_{m=1}^{M}\sum_{n=1}^{N}(K_{ijnm}^{(m)}-K_{ijnm}^{(p)}-K_{ijnm}^{(e)}-\omega^2 M_{ijnm})a_{nm}=0 \qquad i=1,\ldots,N \quad , \quad j=1,\ldots,M \tag{35}$$

By introducing $\mathbf{K}_{NM\times NM}^{(m)}$ as the mechanical stiffness matrix, $\mathbf{K}_{NM\times NM}^{(p)}$ as the piezoelectric layers stiffness matrix, $\mathbf{K}_{NM\times NM}^{(e)}$ as the electrical stiffness matrix, $\mathbf{M}_{NM\times NM}$ as the mass matrix and $\mathbf{A}_{NM\times 1}$ as the matrix of coefficients, Eq. (35) can be expressed in matrix form as:

$$(\mathbf{K}^{(m)}-\mathbf{K}^{(p)}-\mathbf{K}^{(e)}-\omega^2\mathbf{M})\mathbf{A}=0 \tag{36}$$

Hence, the natural frequency of the system (ω) can be obtained, by solving the following equation:

$$det(\mathbf{K}^{(m)}-\mathbf{K}^{(p)}-\mathbf{K}^{(e)}-\omega^2\mathbf{M})=0 \tag{37}$$

5. NUMERICAL RESULTS AND DISCUSSION

5.1. Pull-in Analysis

To apply the numerical solution presented in 4.1, first it is tried to find the best step size of voltage for application of the step by step linearization method and number of grid points for FDM. It can be seen that decreasing of step size of the applied voltage and increasing of number of grid points causes pull-in voltage changes, up to a point where desired accuracy is satisfied and after that, by changing the step size of applied voltage and number of grid points, pull-in voltage remains constant. Based on the obtained results, the optimum step size of applied voltage and grid points may be taken account as $0.1V$ and 21×21, respectively.

The geometrical and material properties of multilayer microplate are listed in Table 1.

Results show that when the applied voltage reaches the specific value, the microplate is pulled into the fixed electrode suddenly and in fact, divergence instability or Pull-in a phenomenon occurs.

Francais and Dufour [31] measured the center deflection of a square fully clamped, under various electrostatic actuations. In figure 2, we compare the deflection at the center of the plate which calculated by using our proposed model for the case of no residual stress effect and piezoelectric layers with the experimental results obtained by Francais and Dufour. As it is seen, there is a good agreement.

Figure .3 shows that residual stress has considerable effect on Pull-in phenomena. The tensile residual stress increases the pull-in voltage and the compressive one decreases it.

Figures 4, 5, 6 and 7 show the obtained pull-in voltages for different applied voltages to piezoelectric layers with various residual stresses and micro plate sizes. The pull-in voltage can be controlled by applying different voltages to the piezoelectric layers.

As it is shown in Figures 4 and 5, increase in negative applied voltage to the piezoelectric layers increase the pull-in voltage. As the matter of fact, the effect of negative applied voltage to the piezoelectric layers on the pull-in voltage is the same as the effect of tensile residual stress. Conversely, the increase in positive applied voltage to the piezoelectric layers, as it is shown in figures 6 and 7, would decrease the pull-in voltage and its influence is like the compressive residual stress effect.

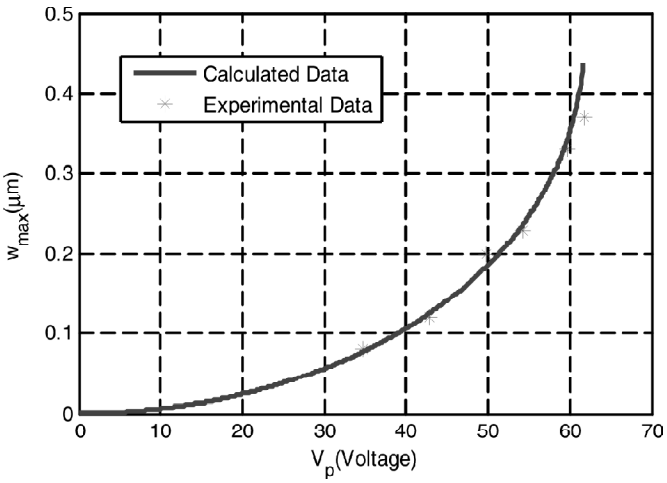

Figure 2: Center Deflection Versus Applied Voltage ($a = b = 250\mu m$)

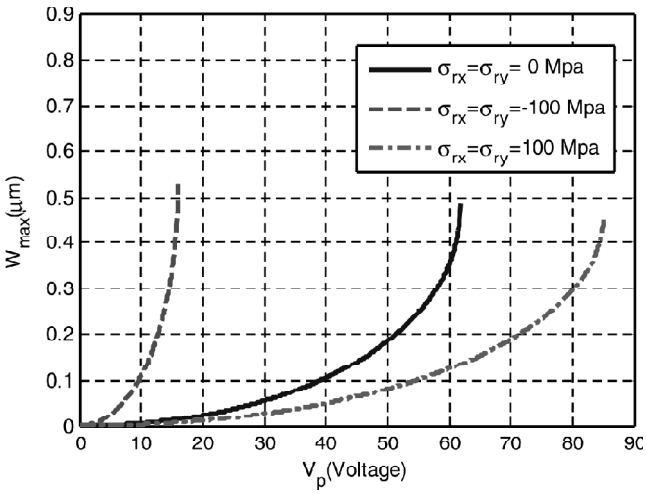

Figure 3: Center Deflection Versus Applied Voltage for Different Residual Stresses ($a = b = 250\ \mu m$)

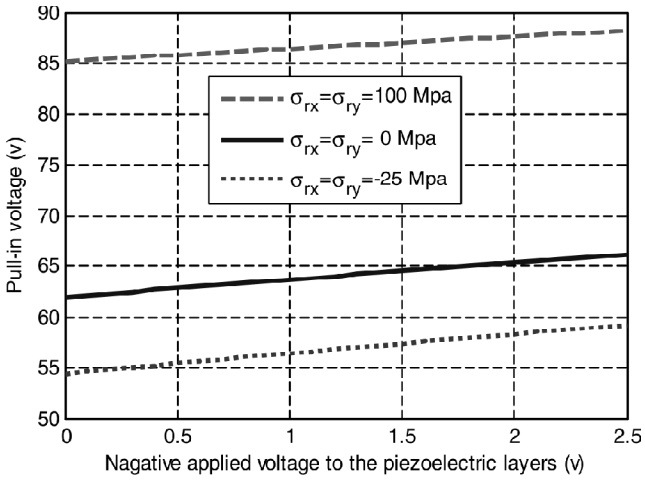

Figure 4: Pull-in Voltage Versus Negative Applied Voltage to the Piezoelectric Layers for three Different Values of Residual Stress (a = b = 250μm)

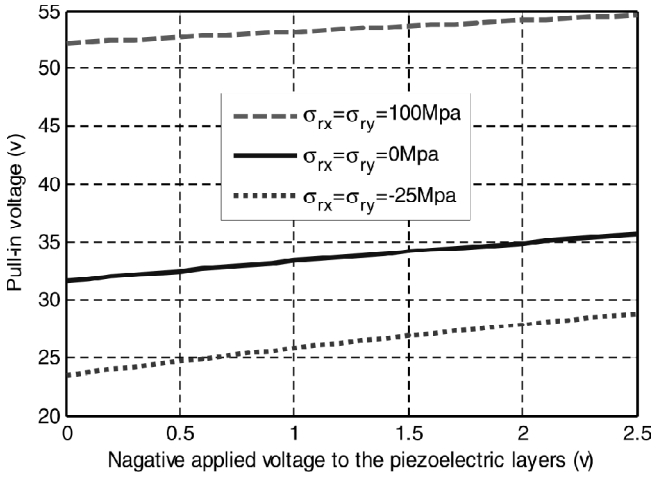

Figure 5: Pull-in Voltage Versus Negative Applied Voltage to the Piezoelectric Layers for three Different Values of Residual Stress (a = b = 350 μm)

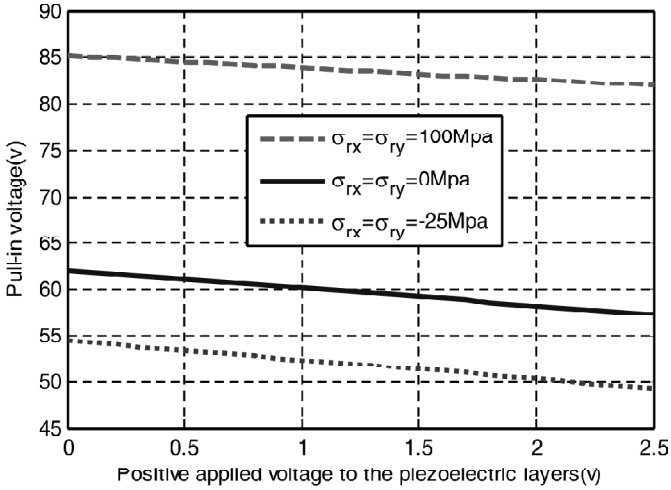

Figure 6: Pull-in Voltage Versus Positive Applied Voltage to the Piezoelectric Layers for three Different Values of Residual Stress (a = b = 250 μm)

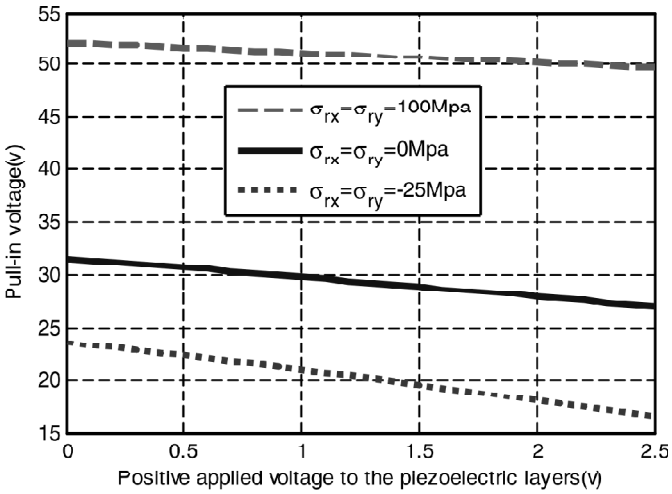

Figure 7: Pull-in Voltage Versus Positive Applied Voltage to the Piezoelectric Layers for three Different Values of Residual Stress (a = b = 350 μm)

In all of the presented figures, the effect of piezoelectric force is more significant when applied to the microplates with compressive residual stresses.

5.2. Eigen Frequency Analysis

In this paper, w_b was selected as the basis function in Eq. (24). By this consideration and applying the solution method presented in 4.2, the first natural frequency of the system can be calculated.

Figures 8 and 9 show the natural frequency-applied voltage curve for various applied voltages to piezoelectric layers and micro plate sizes. It can be seen that with increasing the applied voltage to the micro plate, the natural frequency of the micro plate decreases and approaches to zero in the pull-in voltage. It indicates that applying the negative voltage to piezoelectric layers increases the natural frequency of the system and the positive voltage decreases it.

Figures 10, 11, 12 and 13 show the effects of residual stress and voltage of piezoelectric layers on the natural frequency of the microplate. The highest value of natural frequency is introduced for the case of negative applied voltage and tensile residual stress.

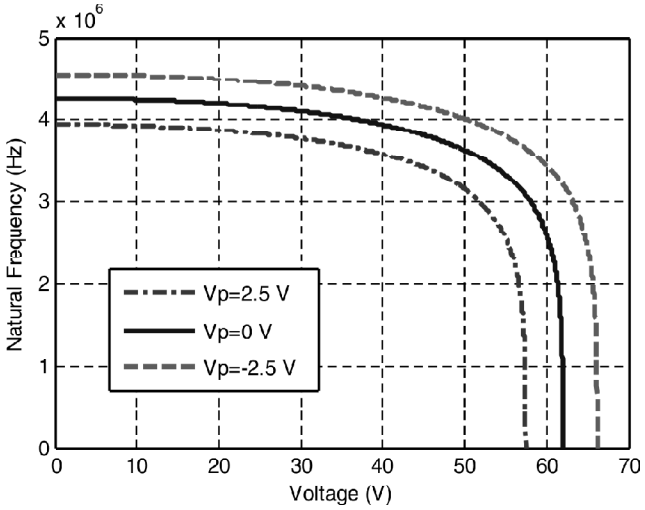

Figure 8: Natural Frequency Versus Applied Voltage for three Different Values of Applied Voltage to the Piezoelectric Layers (a = b = 250 μm)

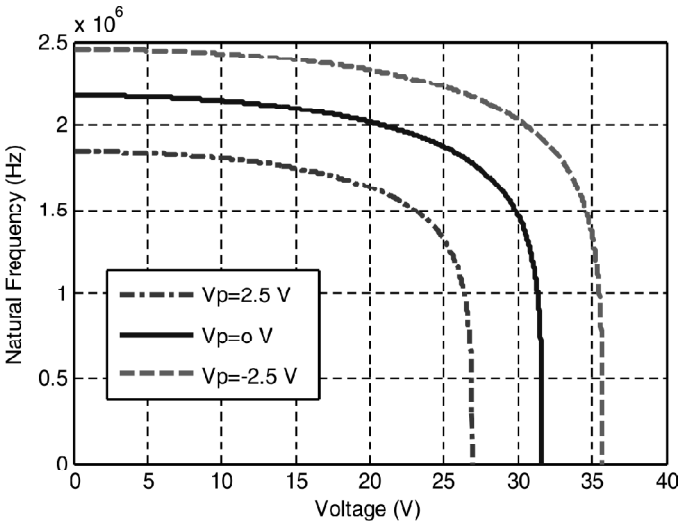

Figure 9: Natural Frequency Versus Applied Voltage for three Different Values of Applied Voltage to the Piezoelectric Layers (a = b = 350 μm)

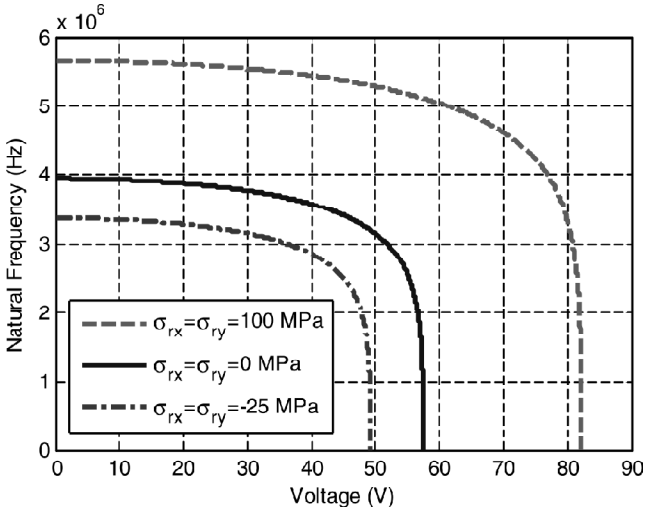

Figure 10: Natural Frequency Versus Applied Voltage for three Different Values of Residual Stress (a = b = 250 μm, Vp = 2.5 V)

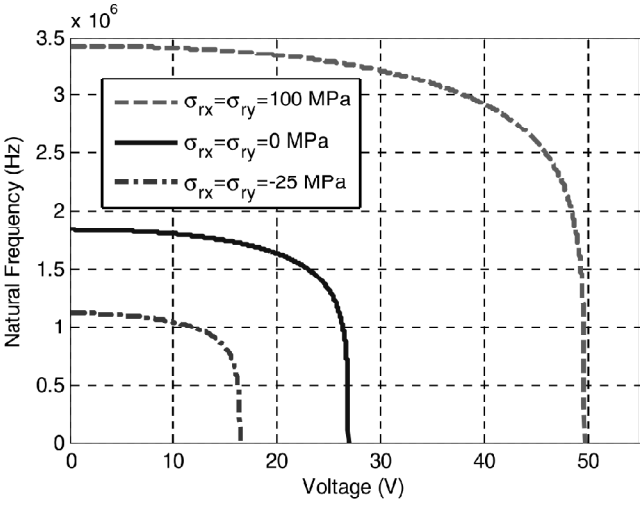

Figure 11: Natural Frequency Versus Applied Voltage for three Different Values of Residual Stress (a = b = 350 μm, Vp = 2.5V)

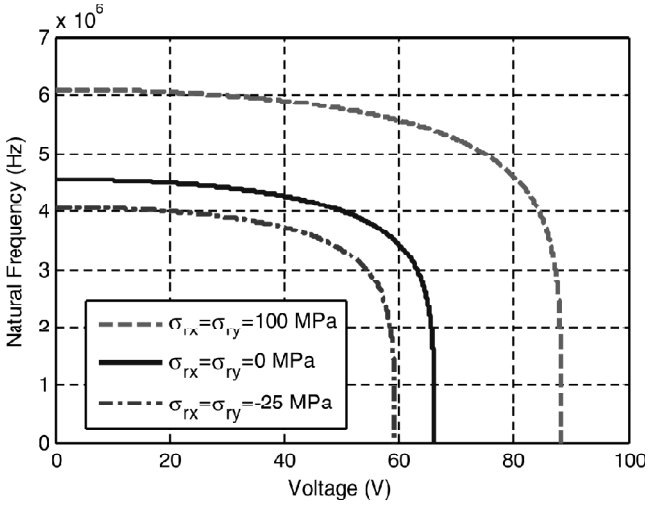

Figure 12: Natural Frequency Versus Applied Voltage for three Different Values of Residual Stress (a = b = 250 µm, V_p = –2.5 *V*)

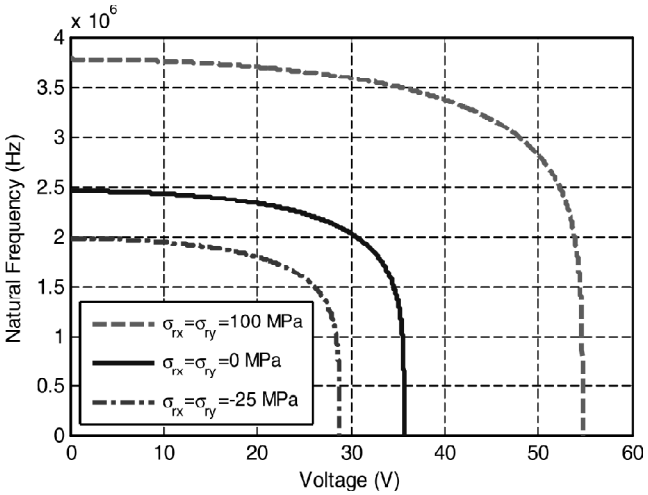

Figure 13: Natural Frequency Versus Applied Voltage for three Different Values of Residual Stress (a = b = 350 µm, V_p = –2.5 *V*)

Table 1
Geometrical and Material properties of Micro-plate

	Center layer	*Piezoelectric layers*
Thickness	3µm	0.01µm
Young's modulus	169Gpa	78.6Gpa
Poisson's ratio	0.06	0.3
$\overline{e}_{31}, \overline{e}_{32}$	–	–9.29 I/m^3
G	1 µm	–
ε_0	8.854187×10^{-12} F/m	–

6. CONCLUSION

By using of a mathematical formulation with deriving governing nonlinear differential equation and a numerical solution, static behavior and eigen frequency of an electrostatically actuated rectangular microplate with pair of surface-bonded piezoelectric layers were studied. The pull-in voltage of the microplate considering different design parameters by using of step by step increasing electrostatic force was calculated. A numerical algorithm was developed to evaluate the eigen frequency of the model and was shown that with increasing the voltage, applied to the electrostatic electrodes natural or eigen frequency of system converges to zero in the vicinity of pull-in voltage. It means that the pull-in instability is a divergence or an Euler buckling strut.

The advantages of piezoelectric and electrostatic mechanisms were combined to achieve wide tuning range for the resonance or natural frequency of the microplate. By applying a DC voltage to the electrostatic electrodes, eigen frequency only could be decreased but by applying a positive or negative dc voltage to the piezoelectric layers eigen frequency could be decreased or increased. The obtained results also can be used in micro accelerometers and resonators for controlling the sensor stable region, bandwidth or sensor sensitivity.

References

[1] Teymoori M, Abbaspour-Sani E, Design and Simulation of a Novel Electrostatic Peristaltic Micromachined Pump for Drug Delivery Application. *Sens Actuators A* 2005; 117: 222–229.

[2] M. T. A. Saif, B. E. Alaca and H. Sehitoglu, Analytical Modeling of Electrostatic membrane Actuator Micro Pumps. *J. Microelectromech. Syst.* 1999; 8: 335-345.

[3] Zhang Y., Gu P., Fan X., Progress on Research of MEMS-Based Micropump 7th International Conference on Electronic Packaging Technology, 2006. ICEPT 06.

[4] J. G. Guo; Y. P. Zhao, Influence of van der Waals and Casimir Forces on Electrostatic Torsional Actuators, *Journal of Microelectromechanical Systems* 2004; 13: 1027–1035.

[5] M. Bao and W. Wang, Future of Microelectromechanical Systems (MEMS), *Sens. Actuators A, Phys.* 1996; 56: 135-141.

[6] J. M. Sallese, W. Grabinski, V. Meyer, C. Bassin, P. Fazan, Electrical Modeling of a Pressure Sensor MOSFET, *Sens. Actuators A, Phys.* 2001; 94: 53-58.

[7] Adel Nabian, Ghader Rezazadeh, Ph. D., Mohammadali Haddad-derafshi, Ahmadali Tahmasebi, Mechanical Behavior of a Circular Micro Plate Subjected to Uniform Hydrostatic and Non-uniform Electrostatic Pressure, *J. Microsys. Technol.* 2008; 14: 235-240.

[8] R. Zengerle, A. Richter, H Sandmaier, A Micro Membrane Pump with Electrostatic Actuation, In: Micro Electro Mechanical Systems Conference, Travemunde, Germany, 1992: 19-24.

[9] X. M. Zhang, F. S. Chau, C. Quan, Y. L. Lam, A. Q. Liu, A Study of the Static Characteristics of a Torsional Micro Mirror, *Sens. Actuators A, Phys.* 2001; 90: 73-81.

[10] P. P. C. Hsu, C. H. Mastrangelo, K. D. Wise, A High Sensitivity Polysilicon Diaphragm Condenser Microphone, In: MEMS Conference, Heidelberg, Germany, 1998: 580-585.

[11] H. A. Tilmans, R. Legtenberg, Electrostatically Driven Vacuum-encapsulated Polysilicon Resonators: Part II. Theory and Performance. *Sens Actuators A, Phys.* 1994; 45: 67-84.

[12] H. C. Nathanson, W. E. Newell, R. A. Wickstrom, J. R. Davis, The Resonant Gate Transistor, *IEEE Trans. on Elect. Devices* 1967; 14: 117-133.

[13] G. I. Taylor, The Coalescence of Closely Spaced Drops when they are at Different Electric Potentials, In: Proc. Roy. Soc A 306, 1968: 423-434.

[14] Gh. Rezazadeh, A. Tahmasebi, M. Zubtsov, Application of Piezoelectric Layers in Electrostatic MEM Actuators: Controlling of Pull-in Voltage, *J. Microsys. Technol.* 2006; 12: 1163-1170.

[15] P. M. Osterberg, S. Senturia, M-test: A Test Chip for MEMS Material Property Measurement using Electrostatically Actuated Test Structures, *J. Microelectromech. Syst.* 1997; 6:107–118.

[16] W. C. Tang, C. T. C. Nguyen and R. T. Howe, Laterally Driven Polysilicon Resonant Microstructures, *Sens. Actuators* 1989; 20: 25-32.

[17] W. C. Tang, M. G. Lim and R. T. Howe, Electrostatic Comb Drive Levitation and Control Method, *J. Microelectromech. Syst.* 1992; 2: 170-178.

[18] W. S. Lee, K. C. Kwon, B. K. Kim, J. H. Cho, Frequency-shifting Analysis of Electrostatic Tunable Micro-mechanical Actuator, *Journal of Modeling and Simulation of Microsystems* 2001; 2: 83-88.

[19] K. B. Lee, Y. H. Cho, A Triangular Electrostatic Comb Array for MicromechanicalResosant Frequency Tuning, *Sens. Actuators A Phys* 1998; 70: 112-117.

[20] W. F. Faris, E. M. Abdel-Rahman and A. H. Nayfeh, Mechanical Behavior of an Electrostatically Actuated Micropump, In: 43rd AIAA/ASME/ASCE/AHS/ASC Structures, Structural Dynamics, and Materials Conference AIAA 2002-1003, Denver, CO, 2002.

[21] G. W. Vogl and A. H. Nayfeh, A Reduced-order Model for Electrically Actuated Clamped Circular Plates, *J. Micromech. Microeng.* 2005; 15: 684–690.

[22] X. Zhao, E. M. Abdel-Rahman and A. H. Nayfeh, Mechanical behavior of an electrically actuated microplate, In: DETC'03, ASME Design Engineering Technical Conference DETC2003/ VIB-48531.

[23] T. Mukherjee, G. Fedder, J. White, Emerging Simulation Approaches for Micromachined Devices, *IEEE Transactions on Computer-Aided Design of Integrated Circuits and Systems* 2000; 19: 1572-1589.

[24] L. X. Zhang, Y. P. Zhao, Electromechanical Model of RF MEMS Switches, *J. Microsys. Technol* 2003; 9: 420–426.

[25] P. Donthireddy, K. Chandrashekhara, Modeling and Shape Control of Composite Beams with Embedded Piezoelectric Actuators, *J. Composite structures* 1996; 35: 237-244.

[26] R. F. Milsom, N. H. C. Reilly, M. Redwood, Analysis of Generation and Detection of Surface and Bulk Acoustic Waves by Interdigital Transducers, *Trans. on Sonics and Ultrasonics* 1977; 24: 147-166.

[27] P. Quinn, L. Palacios, G. Carman, J. Speyer, Health Monitoring of Structure using Directional Piezoelectric, In: ASME Mechanics and Materials Conference, Blacksburg, 1999.

[28] C. Ugrul, *Stresses in Plates and Shells*, 2nd edition, Mcgraw-Hill, 1999.

[29] H. Sadeghian, Gh. Rezazadeh, and P. M. Osterberg, Application of the Generalized Differential Quadrature Method to the Study of Pull-In Phenomena of MEMS Switches, *J. Microelectromech. Sys.* 2007; 16: 1334-1340.

[30] E. F. Crawley, J. de Luis, Use of Piezoelectric Actuators as Elements of Intelligent Structures, *J. AIAA* 1987; 25: 1373–1385.

[31] O. Francais, I. Dufour, Normalized Abacus for the Global Behavior of Diaphragm: pneumatic, electrostatic, piezoelectric or Electromagnetic Actuation, *J Modeling Simul. Microsys.* 1999; 2:149-160.